Photonic devices based on optical fibers for telecommunication applications

Pantelis Velanas*
National and Kapodistrian University of Athens,
Department of Informatics and Telecommunications,
University Campus, 15784 Athens, Greece
pvelanas@di.uoa.gr

Abstract. In this thesis, all-optical processing for the functionalities of second and third generation optical networks is studied in one hand by means of parametric processes and on the other hand by taking advance of cross phase modulation in highly non-linear optical fibers. Parametric processes are nonlinear effects which arise in optical fibers when high-powered waves are properly placed at proper spectral positions. Through the first part of this thesis an analytical study on the noise characteristics of parametric amplifiers operating at the linear regime is provided taking also into account that the zero dispersion wavelength mapping along fiber's length varies its value. A useful theoretical model for the noise figure estimation is derived, and a comparative study on the noise properties of non-linear fiber with several zero dispersion wavelength mapping is carried out. In the same part of this thesis a 2R polarization insensitive regenerator based on dual pump parametric processes in fiber is proposed and theoretically studied. Two novel fiber based photonic devices, which based on cross phase modulation in highly non-linear fibers, are proposed in the second part of this thesis. The first proposed fiber device is an all optical ultrafast (160 Gbps) reconfigurable (XOR, OR, AND, NAND, OR, NOR, NOT) photonic logic gates and the second device is an all optical ultrafast (40 Gbps) photonic differentiator which has the ability to produce fist-order and second-order temporal derivatives of an optical RZ modulated signal. The fine operation properties of this device have been experimentally demonstrated. Finally the ability of the proposed all optical differentiator to operate as an UWB signal generator has been studied and proven. The proposed all optical UWB signal generator can be used to indoor wireless access network as a last meters solution in next generation optical access networks.

1 Introduction

Within today's Internet, data is transported using optical fiber transmission and wavelength division multiplexing (WDM) systems that today carry a typical 32-80 wavelengths modulated at 2.5 Gbps to 10 Gbps per wavelength. Today's routers and electronic switching systems need to handle almost 0.5 Terabit per second in order to redirect incoming data from fully loaded WDM links. Things become interesting when we consider that the capacity of optical fibers continues to double every 8-12 months. Today's state-of-the-art single fiber capacity exceeds 10 Tbps. Comparing this increase with that of electronic processor speeds which doubles every 18 months (Moore's Law) and comes at the expense of increased chip power dissipation we see

* Dissertation Advisor: Dimitris Syvridis, Professor

that there is a potential bandwidth mismatch in handling capability between fiber transmission systems and electronic routers and switching systems. The story is more complex when we consider that future routers and switches will potentially terminate hundreds or thousands of optical wavelengths and the increase in bit-rate per wavelength will head out to 40 Gbps and beyond to 160 Gbps. Additionally, electronic memory access speeds only increase at the rate of approximately 5% per year, an important data point since memory plays a key role in how packets are buffered and directed through the router. It is not difficult to see that the process of moving a massive number of packets per second (100 million packets/second and beyond the 1 Billion packets/second mark) through the multiple layers of electronics in a router, can lead to router congestion and exceed the performance of electronics and the ability to efficiently handle the dissipated power.

During the last decade, fiber-optic parametric amplifiers (FOPAs) have attracted the interest of many research groups as they are candidates for a great number of all-optical applications such as amplification, wavelength conversion, phase conjugation, 2R regeneration, return-to-zero (RZ) pulse generation, optical time-division demultiplexing, all-optical sampling and all-optical switching. The above FOPA applications are mainly demonstrated using one or two high-power pump waves which are launched together with a signal in a highly nonlinear dispersion shifted fiber (HNL-DSF). The HNL-DSF's high nonlinearity along with high input power ensures a large four wave mixing (FWM) efficiency, while HNL-DSF's low dispersion slope ensures a broadband FWM efficiency. Furthermore, the operation properties of the photonic fiber devices which based on cross phase modulation (XPM) in HNL-DSFs are also in high interests because they have the ability to operate in high bit rates, offering a wide number of ultrafast all optical subsystems. The thesis is structured as follows. In the second section a 2R all optical regenerator is proposed which takes advance on a dual pump FOPA's polarization insensitive properties and the impact of fiber's dispersion fluctuation on noise characteristics of an one pump FOPA is analyzed in the third section. In the last section two novel ultrafast photonic fiber devices are proposed. The operation of these devices is based on the XPM in HNL-DSFs.

2 2R all optical polarization insensitive regenerator

Modern optical communication systems require not only signal amplification periodically but also devices that are capable of ultrafast, all optical, signal processing. As channel line rates in optical networks become faster, penalties from dispersion, polarization mode dispersion (PMD) and nonlinearities in optical fiber become more sever. Long-haul propagation in systems operating at high channel rates will require ultrafast regeneration that re-amplifies, reshapes and retimes the optical signal (3R-regeneration). Fiber-optic parametric amplifiers (FOPAs), based on four wave mixing (FWM) occurring inside optical fibers, are attracting considerable attention because they can provide broadband amplification and can, thus, replace erbium-doped fiber amplifiers commonly used for signal amplification. However, FOPAs are also an ideal candidate for ultrafast, all optical, signal processing because of the instantaneous response of the silica nonlinearity responsible for FWM in optical fibers. Moreover, polarization-independent operation is a vitally important

feature for optical components in communication systems. Common FOPAs are not polarization-independent, thus they need to be modified in order to become polarization independent. Recently a novel method has been presented for obtaining a FOPA with gain independent of signal's SOP based on the use of two orthogonal pumps [1]. Our work [2] is based on this technique and it is found that it provides the ability to a FOPA to operate as a polarization-independent 2R regenerator as it will be described in the next section.

A schematic of the proposed FOPA-based regenerator is shown in Fig. 1. Two amplified, through erbium doped fiber amplifiers (EDFAs), continuous wave (CW) orthogonally polarized pumps, which are positioned at 1535 nm and 1585 nm, respectively, are coupled and launched into the highly non linear fiber (HNLF). The power of the pumps is set to be equal to +24 dBm. At the same time, a return to zero (RZ) modulated signal, which is placed at 1565.4 nm, is inserted into the HNLF in order to interact with the co-propagated pumps along the fiber's length. The considered 1 km length HNLF has a nonlinear coefficient equal to 17 W^{-1} / km and the dispersion slope is set to be equal to 0.02 ps^2/nm/km.

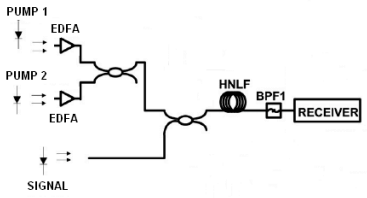

Fig. 1. Schematic of the proposed 2R all optical regenerator architecture

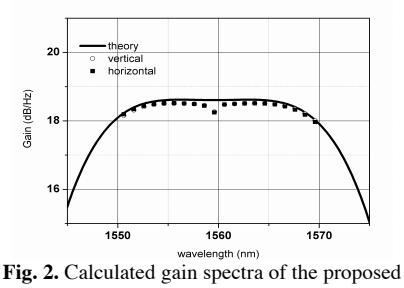

Fig. 2. Calculated gain spectra of the proposed FOPA

The verification of the theoretically prediction of the polarization-independent operation of our device has been performed following the same procedure, which has been already described in [1]. The gain of the proposed FOPA is analytically and numerically calculated (Fig. 2). As it is clearly shown from Fig. 2 the FOPA's gain doesn't depend on the signal's state of polarization.

In order to study the operation properties of the proposed polarization insensitive regenerator, the dependence of the output peak power as a function of the input peak power is calculated and presented in Fig. 3(left) for several SOPs of the input signal. The PMD of the HNLF is neglected, considering that nowadays there are state-of-the-art HNLFs with almost zero PMD coefficient. According to fig. 3 (left), the output signal power is common for all studied SOPs for input signal powers up to a couple of mW (linear regime). At higher input power levels, the output power varies up to 3dB depending on the input SOPs meaning that the FOPA is not polarization independent in the saturation regime. The behavior is due to the growth of higher order FWM spectral components, which are dependent on the relation between signal's and pumps' polarization state. Specifically the higher order products are maximized when the input signal SOP has a $\pi/4$ angle with respect to the two pumps polarizations. In

that case the signal gain is reduced and transferred to the higher order products. On the other hand, when the SOP of the input signal takes values different from 45^0 the emergence of higher order products is less intense. Although the shape of the power transfer function and the exact amount of the output power is determined by the input signal polarization state, all the transfer functions depicted in fig. 3(left) have the desired S-shape needed for the suppression of noise at logical level "1". In order to have the maximum possible performance for all different transfer functions, the input signal power must be set to 6mW (Fig. 3(left)). For lower or higher power values the operation of the 2R regenerator is significantly favored for specific input SOPs and respectively degraded for other ones.

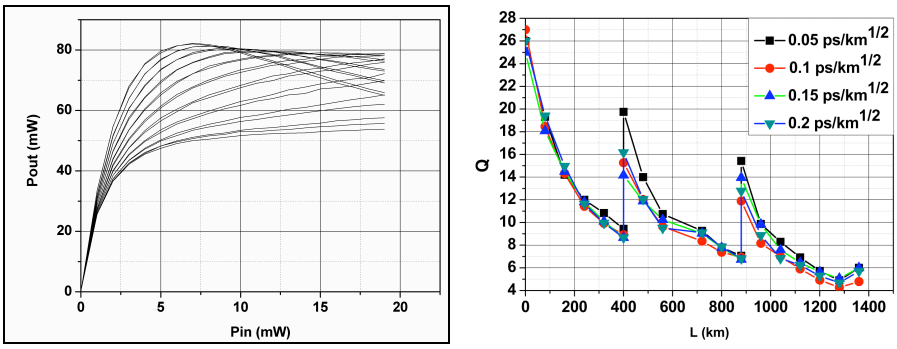

Fig.3. Power transfer characteristics of the polarization- independent regenerator for several signal's SOP (left) and Q-factor of the transmitted signal as a function of the distance when the repeater is placed at every 5 spans (right)

The performance of the proposed regenerator is numerically evaluated, for a 40 Gb/s RZ signal which is propagated through a link which consists of similar transmission segments containing a single mode fiber (SMF), a dispersion compensating fiber (DCF), an EDFA and an OBPF having 3-dB bandwidth equal to 1 nm., in terms of the calculation of the Q factor of the output signal for several values of the PMD coefficient in the optical link. The reshaping device is placed every after five transmission segments which correspond to 400 km of SMF. The employment of the reshaping device every 400 km enhances the transmitted signal characteristics resulting in adequate performance (Q>6) for distances longer than 1000 (Fig. 3 (right)).

3 Impact of dispersion fluctuations on noise properties of single pump FOPA

The noise characteristics of single-pump FOPAs have been theoretically investigated [3] for a lossless undepleted FOPA neglecting the dispersion fluctuation effect. In practice, highly non linear-dispersion shifted fibers (HNL-DSFs) have random longitudinal dispersion fluctuations. The FWM is sensitive in random changes of the zero dispersion wavelength (ZDWL) occurring along the fiber, and thus the parametric process is unavoidably affected. These effects become more evident when the pump wavelength is positioned close to the ZDWL, as it is

necessary in order to obtain broader gain bandwidth. In this work the FOPA noise performance is investigated in the case that ZDWL is varying along the fiber for a lossless and undepleted quantum-limited single-pump FOPA. The main noise sources affecting the FOPA performance are the amplified quantum noise (QN) and the noise characteristics of the pump wave. QN is related to the vacuum fluctuations that take place in the fiber, due to the quantization of the optical light, which result in the existence of optical power, even though there are no signal photons. On the other hand the pump noise characteristics, which correspond to the level of pump intensity variations, affect the signal and the idler wave intensity through the FWM process. The pump wave is much less influenced by the quantum noise which can be neglected. The most indicative criterion for the amplifier noise performance is the value of its noise figure. The noise figure is defined as the ratio of the input signal-to-noise ratio (SNR_{in}) to the output signal-to-noise ratio (SNR_{out}). In our work, the noise figure is calculated assuming that the input electrical signal to noise ratio ($ESNR_{in}$) is limited only by the shot noise at detection. The noise figures for both the signal and the idler waves, using are defined as [3]:

$$NF_j = \frac{2G_s - 1}{G_j} + \frac{\sigma^2_{j-Pp}}{G_j^2 4R_j S_{QN} P_s(0)\Delta f} \tag{18}$$

The theory for the FOPA gain and noise characteristics is valid for the case that the ZDWL remains constant along the fiber[4]. In real fibers, the ZDWL varies along the fiber length as a result of imperfections during the drawing process or due to the sensitivity of the material in external conditions such as temperature. The former is responsible for short scale fluctuations of ZDWL, while the latter causes long scale fluctuations. Taking into account the fluctuations of the ZDWL, the analytical expressions for the FOPA gain and the *NF* do not apply anymore. The fact that the ZDWL varies randomly along the fiber length makes the gain and the noise figure random processes in terms of ZDWL. Therefore, the amplifier gain and *NF* characteristics can be only studied statistically. In the literature, average gain characteristics under the ZDWL variation regime have been analytically and numerically investigated for both single pump and dual pump FOPAs. The noise figure has not been assessed in this regime up to now. Due to the stochastic nature of the ZDWL variations, it is quite complicated to derive analytical expressions for the average value of the *NF*. Instead of it, it is feasible to derive the average *NF* numerically. This can be achieved by averaging the noise figures calculated for a number of unique fiber realizations. The dispersion fluctuations are directly related to the statistics of the random longitudinal ZDWL values. In the specific work, the zero-dispersion wavelength λ_0 is modeled as a sum of a constant and a randomly varying part, where the constant part is the mean zero dispersion wavelength value and the randomly varying part is a real Gaussian stochastic process.

The Gaussian process has zero mean value and the standard deviation indicates the amount of ZDWL variations which are assumed to happen periodically. The variation period of the λ_0 is l_p = 5m. The average value of the gain and the noise figure are estimated numerically for a number of fibers having a unique longitudinal sequence of ZDWL values. In order to examine the accuracy of our method, we have compared

it to the NLSE in terms of the noise figure estimation. At first, we consider a particular FOPA implementation, by choosing a specific ZDWL map, where dispersion fluctuations follow a Gaussian stochastic process with standard deviation σ_λ=2nm. The optical signal power launched into the amplifier is -10dBm. The gain and noise figure characteristics of the specific FOPA are calculated either by numerically simulating the NLSE, or the three-coupled propagation equations. It is worth-mentioning that the latter was 20 times faster than the numerical integration of NLSE based on the SSF method and hence has been preferred for the derivation of the results of this thesis.

In Fig. 4 (left) the <*NF*> and the average gain <*G*> are illustrated versus the amplifier bandwidth for a variety of FOPA gains. Two standard deviation values describing the ZDWL fluctuations have been considered (1nm, 2nm) for 300 unique random fiber realizations in each case. Moreover the case corresponding to constant dispersion characteristics is also included. The input signal power is -10 dBm. According to fig. 4 (left), ZDWL variations tend to reduce the FOPA gain, increase the noise figure around the spectral region of the peak gain and decrease it around the spectral region of its theoretical maximum value. Under the dispersion fluctuations regime the average gain peak is transferred at wavelengths closer to the pump wave, where the phase matching $\Delta\varkappa$ condition is better satisfied. The latter is more evident when higher pump powers are utilized for gain maximization. In that case, the phase matching is satisfied for higher pump-signal wavelength spacing values which increase the sensitivity of the parametric process in dispersion fluctuations.

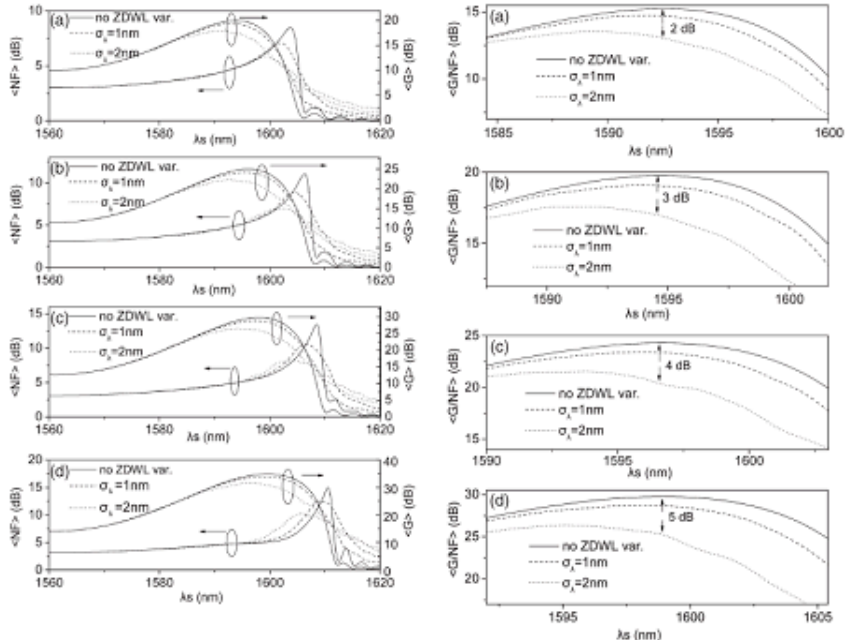

Fig.4. (left) Average noise figure <*NF*> and average gain <*G*> versus signal wavelength and (right) average value of gain-to-NF ratio, in terms of the 3-dB bandwidth, for different values of dispersion fluctuations for different FOPA implementations with peak gain of (a) 20, (b) 25, (c) 30, and (d) 35 dB

The noise figure behavior can be analogously explained taking also into account that it grows rapidly at the outer part of the gain spectrum. In the case that the signal is positioned at a spectral region around the original gain peak wavelength, the dispersion fluctuations will statistically increase the noise figure of the amplifier as the maximum gain point is transferred at wavelengths closer to the pump wave. The impact of random ZDWL variations is more significant for higher gain FOPAs, where stronger pump waves are required. On one hand, the higher pump power increases the noise figure of the amplifier regardless of the ZDWL variations influence. On the other hand, the spectral region around the gain peak lies at wavelengths apart from the pump wave where the $\Delta\beta$ fluctuations increase affecting both the gain and the noise properties of the FOPA. The maximum noise figure is statistically reduced when the ZDWL variations are included (fig. 4 (left), dotted and dashed lines) compared to the case that dispersion is longitudinally constant. This is attributed to the fact that the maximum noise figure is positioned at a different wavelength for each fiber characterized by a unique λ_0 longitudinal evolution.

The evaluation of the FOPA performance under the ZDWL fluctuations can be much better accomplished by introducing the gain-to-noise figure ratio (*G*/*NF*). The parameter *G*/*NF* can satisfactorily describe the performance of an amplifier device, quantifying the interplay between gain and noise figure characteristics. The mean *G*/*NF* value is depicted in fig. 4 (right), where it is shown that the degradation of the ratio *G*/*NF* is less significant for FOPAs providing moderate gains (≈20dB). On the contrary, the parameter *G*/*NF* is much influenced by the dispersion fluctuations when high-gain FOPAs are considered. In the case of moderate gains, the peak gain of the amplifier decreases due to the random disturbance of phase-matching condition, while the noise figure characteristics are less impaired. This justifies the 2.2dB difference between the *G*/*NF* of a FOPA with constant ZDWL and the FOPAs characterized by 2nm ZDWL fluctuations. On the other hand, at higher gains (>25 dB), the effect of dispersion fluctuations influence significantly both the gain and the noise properties of the FOPA, and thus the parameter *G*/*NF* is much more degraded (5dB) especially in the case that 2nm fluctuations of the ZDWL are considered.

The preceding analysis has not taken into account the impact of the input signal power on the noise performance of FOPAs in the special case of dispersion fluctuations. In that case noise figures are lower compared to those corresponding to a signal power of -10dBm, while the gain remains constant in terms of the two signal powers. Nevertheless, the noise figure increase around the gain peak in the case of pronounced dispersion variations (σ_λ=2nm) is once more observed and it can be up to 0.5dB compared to the case of a FOPA with constant dispersion characteristics.

4 Ultrafast photonic devices based on cross phase modulation in fibers

In this section the operation features of a 160Gb/s reconfigurable all-optical logic gate based on cross phase modulation in highly nonlinear fibers are numerically investigated for six logic functions (XOR, OR, NAND, NOR, NOT and AND). High bit rate operation is numerically demonstrated for a wide input signal wavelength range (>20nm) [5, 6]. Performance enhancement of the proposed setup operating at 160Gb/s for different signal wavelengths is exhibited by using a 2R regenerator based

on the self-phase modulation effect in highly nonlinear fibers at the gate's output. The operation of the multi-functional logic gate is investigated considering either a pulsed or a continuous wave probe. The filter's position, the probe's spectrum broadening characteristics, and the high sensitivity to parameters such as the input signals' power and the exact adjustment of the time delays between the input waves (data signals) play a crucial role in the performance of the reconfigurable gate. The replacement of the clock probe with a CW probe can make the device much more insensitive to initial time delays sacrificing three logical operations (NOR, NOT, NAND). In order to dynamically assess the proposed all-optical reconfigurable logic scheme, numerical simulations based on the nonlinear Schrödinger equation (NLSE) using the split-step Fourier (SSF) method have been carried out, accounting for up to the fourth-order dispersion. The complete model described in takes also into account the four-wave mixing (FWM) interaction and the Raman effect neglected by the theory (fig. 5).

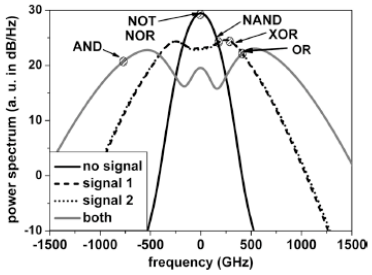

Fig.5. Spectral broadening of the probe wave due to XPM. The circles indicate the positions where the filter must be tuned for the operation of each logical gate.

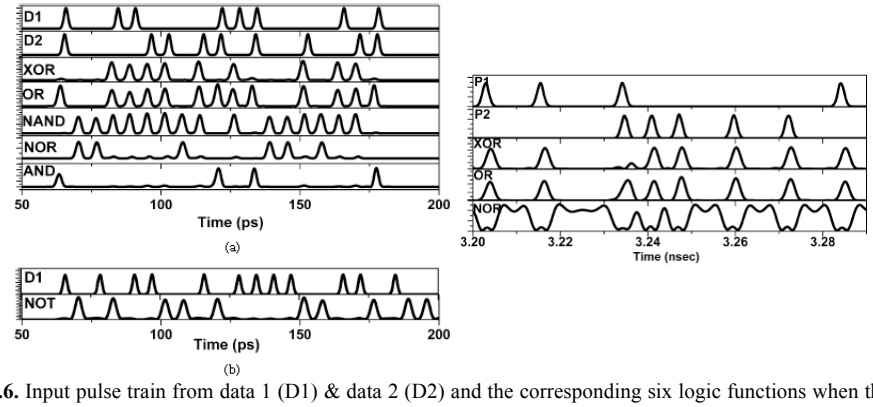

Fig.6. Input pulse train from data 1 (D1) & data 2 (D2) and the corresponding six logic functions when the probe is a pulsed signal (left) and the output after XOR, OR, and NOR operation when the probe is a CW. The output signal for NOR operation is non-return-to-zero one (right).

Furthermore, an ultrafast all-optical differentiator generating the first- and the second-order temporal derivative of the intensity of optical signals is presented in this thesis [7]. Differentiation is obtained via an optical fiber that plays the role of an optical phase modulator, an optical bandpass filter and a photodetector. The operation of the proposed device is theoretically studied in order to highlight significant parameters

that affect the performance of the differentiator, namely the filter transfer function, the power of the propagating waves and the fiber characteristics (length and nonlinear coefficient).

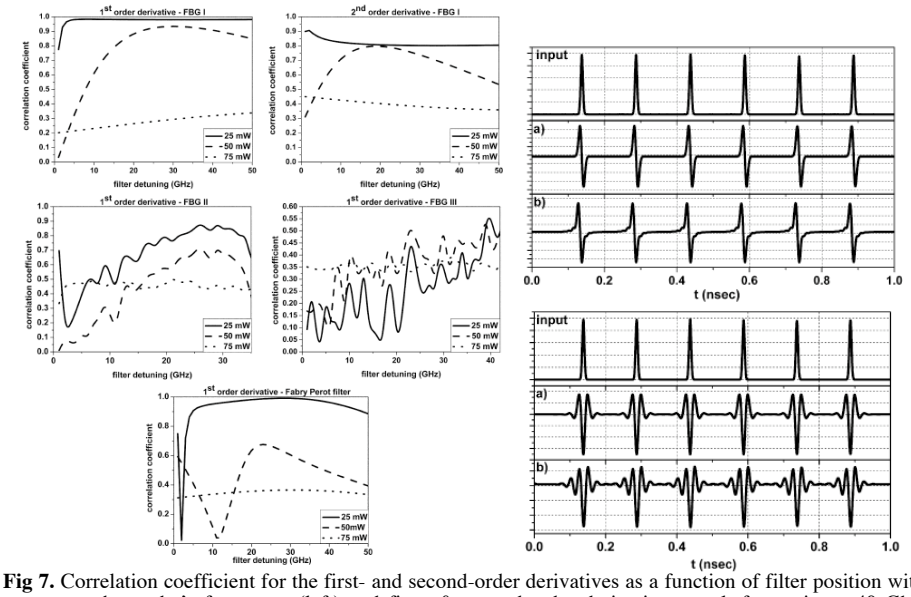

Fig 7. Correlation coefficient for the first- and second-order derivatives as a function of filter position with respect to the probe's frequency (left) and first- & second-order derivatives result for an input 40 Gb/s Gaussian pulse train, (a) as they are theoretically predicted and (b) numerically calculated (right)

The comparison between the numerically calculated derivatives and the theoretically expected ones is performed by estimating the correlation coefficient between them. According to the numerical analysis, high correlation coefficients can be achieved in certain operating regimes. The same device can be utilized in order to produce ultrawideband (UWB) impulse signals [7, 8]. Electrical monocycle or doublet pulses can be obtained at the output of the photodetector (PD) using the proper tunable optical filter. Experimental verification of the theoretically predicted and numerically calculated results is finally presented for high bit-rate signals.

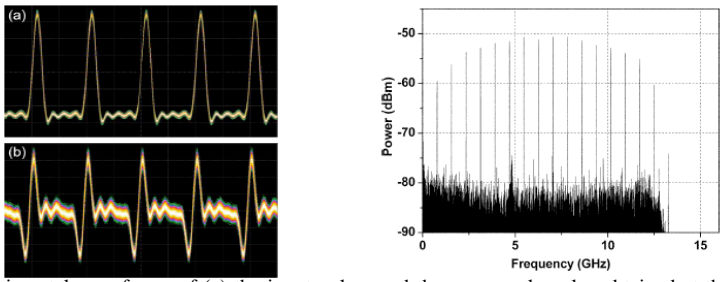

Fig 8. Experimental waveforms of (a) the input pulses and the monocycle pulse obtained at the output of the PD (left) and the power spectrum of the shaped 12.5 Gb/s signal obtained at the photodiode's output (right)

5 Conclusions

Theoretical, numerical and experimental results regarding the performance of photonic devices based on in terms of offering broadband amplification, all-optical regeneration, all optical logic functions and all-optical differentiation have been presented. A theoretical model for the estimation of the impact of fiber's dispersion fluctuation on the noise features of parametric amplifiers was derived. A polarization insensitive reshaping schemes based solely on FWM and parametric amplification in optical fibers were numerically demonstrated. Finally, a reconfigurable photonic logic gate and an all-optical differentiator based on cross phase modulation in highly non linear fibers was numerically and partly experimentally tested providing promising results. These schemes are very robust in terms of the bit rate transparency (>40Gbps).

References

1. K. K. Y. Wong, M. E. Marhic, K. Uesaka, L. G. Kazovsky: Polarization-independent two-pump fiber optical parametric amplifier, vol. 14, IEEE Photon. Technol. Lett, (2002), 911-913.
2. P. Velanas, A. Bogris, D. Syvridis: Polarization-Insensitive 2R- regenerator based on two-pump fiber optical parametric amplifier, IEEE Winter Topicals 2009 Parametric Amplification II 12-14 January 2009.
3. P. Kylemark, P. O. Hedekvist, H. Sunnerud, M. Karlsson, and P. A. Andrekson: Noise characteristics of fiber optical parametric amplifiers, vol. 22, IEEE J. Lightwave Technol., (2004), 409-416.
4. P. Velanas, A. Bogris, D. Syvridis: Impact of dispersion fluctuations on the noise properties of fiber optic parametric amplifiers, vol 24, IEEE J. Lightwave Technol. (2006),2171-2178.
5. A. Bogris, P. Velanas, D. Syvridis: Numerical investigation of a 160 Gb/s reconfigurable photnic logi gate based on cross phase modulation in fibers, vol. 19, IEEE Photonic Technol. Letters (2007), 402-404.
6. P. Velanas, A. Bogris, D. Syvridis: Operation properties of a reconfigurable photonic logic gate based on cross phase modulation in highly non linear fibers, vol. 15, Elsevier, Fiber Optical Technology (2009), 65-73.
7. P. Velanas, A. Bogris, A. Argyris, D. Syvridis: High speed all-optical first- and second-order differentiators based on cross phase modulation in fibers, vol. 26, IEEE J. Lightwave Technology (2009), 3269-3276.
8. P. Velanas, A. Bogris, A. Argyris, D. Syvridis: Ultrawide-Band pulse generation based on cross phase modulation in fibers, IEEE Winter Topicals 2008, Nonlinear Photonics (2008), 90-91.